NUMERICAL SIMULATION FOR THE SINGLE-BUBBLE ELECTROSPINNING PROCESS

by

Lan XU [a,b*]***, Jiang-Hui ZHAO*** [a,b]***, and Hua LIU*** [c,d]

[a] Nantong Textile Institute, Soochow University, Nantong, China
[b] National Engineering Laboratory for Modern Silk, College of Textile and Clothing Engineering, Soochow University, Suzhou, China
[c] College of Textile and Costume, Yancheng Institute of Industry Technology, Yancheng, China
[d] Jiangsu R&D Center of the Ecological Textile Engineering and Technology, Yancheng Institute of Industry Technology, Yancheng, China

Original scientific paper
DOI: 10.2298/TSCI1504255X

This paper studies numerically the two-phase flow in the single-bubble electrospinning process by solving the modified Navier-Stokes equations under the influence of electric field, and the interface between the two fluids has been determined by using the volume of fluids method. A realizable k-ε model is used to model the turbulent viscosity. The numerical results offer in-depth insight into physical understanding of many complex phenomena which cannot be fully explained experimentally.

Key words: *bubble-electrospinning, two-phase model, numerical simulation, computational fluid dynamics techniques*

Introduction

Bubble-electrospinning is a multi-phase and multi-physics process involving fluid dynamics, electrohydrodynamics, mass and heat diffusion, and transfer, *etc*. During the bubble-electrospinning process, an electric field presented induces charged into the polymer bubble surface, and quickly relax to the bubble surface. The coupling of surface charge and the external electric field creates a tangential stress, resulting in the deformation of the bubble. Once the electric field exceeds the critical value needed to overcome the surface tension, the bubble is broken, and the ruptured bubble is pulled upwards to form a charged jet, which is then received on the metal receiver as nanofibers [1-3], fig. 1.

Many experimental and theoretical studies have been conducted to understand the bubble-electrospinning process and some simplified theoretical models have been presented for research mechanical mechanism of the process [1-5]. He [1] modeled surface tension of bubble and bubble hierarchical rupture. He, et al. [3] established the allometric relationship between jet and bubble [4]. Dong, *et al.* [4] and Wilson *et al.* [5] analyzed the potential distribution around the bubble. However, almost all objects of these studies are single-phase flow, and cannot offer in-depth insight into physical understanding of many complex phenomena which can not be fully explained experimentally.

* Corresponding author; e-mail: lanxu@suda.edu.cn

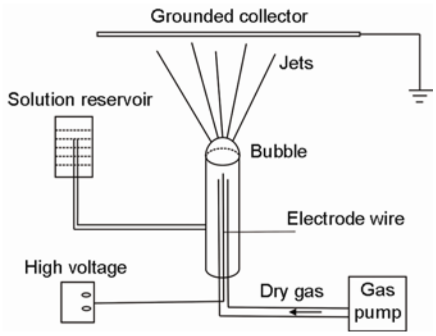

Figure 1. Single-bubble electrospinning set-up

This paper numerically studies the two-phase flow in the single-bubble electrospinning process by applying computational fluid dynamics (CFD) techniques to gain significant insight and a better understanding of the process, fig. 1. The two-phase flow can be calculated by solving the modified Navier-Stokes equations under the influence of electric field and the interface between the two fluids has been determined by using the volume of fluids method. The CFD simulation results show the effects of various single-bubble electrospinning parameters, such as voltage and flow rate, on quality of product, and can be used to optimize and control the electrospinning parameters.

Model

The dynamics of air and polymer solution in the single-bubble electrospinning process are modeled by CFD techniques. To simulate the mechanism of such two-phase flow, numerical CFD sub-model development can be categorized into three main components, magnetohydrodynamics (MHD) model [6], turbulent model [7], and volume of fluid (VOF) model [8, 9].

The MHD Model

Electromagnetic fields are described by Maxwell's equations [6]:

$$\frac{\partial q_e}{\partial t} + \nabla J = 0 \tag{1}$$

$$\nabla \times \vec{\mathrm{E}} + \frac{1}{c}\frac{\partial \vec{\mathrm{B}}}{\partial t} = 0 \tag{2}$$

$$\nabla \vec{\mathrm{H}} - \frac{1}{c}\frac{\partial \vec{\mathrm{D}}}{\partial t} = \frac{1}{c}\vec{\mathrm{J}} \tag{3}$$

where q_e is the electric charge, $\vec{\mathrm{E}}$ – the electric field, $\vec{\mathrm{J}}$ – the current, $\vec{\mathrm{B}}$ – the magnetic induction, $\vec{\mathrm{H}}$ – the magnetic field, $\vec{\mathrm{D}}$ – the atomic displacement vector, and c – the velocity of light in a vacuum ($c = 2.998925 \pm 0.00006 \cdot 10^8$ m per second).

In this paper, the approach for the current density is to solve the electric potential equation and calculate the current density using Ohms law. With the knowledge of the induced electric current, the MHD coupling is achieved by introducing additional source terms to the fluid momentum equation and energy equation.

Turbulent model

The k-ε turbulent model is applied to deal with turbulent flows in strong electric fields. The Reynolds time-mean equations for continuity and momentum are of the same form as governing equations if transient quantities are replaced by time-mean quantities. But the stress tensor in turbulence includes an extra contribution from eddy viscosity besides the part due to molecular viscosity [7].

It is a two-equation eddy viscosity model with the following specification:

$$\mu_t = \rho \nu_t, \qquad \nu_t = C_\mu \frac{k^2}{\varepsilon}$$

where C_μ is a constant (with a typical value 0.09), k – the turbulent kinetic energy, and ε – the rate of dissipation of turbulent kinetic energy. They can be determined by solving transport equations.

The VOF model

The VOF model [8], which attempts to track the interface based on the mass conservation, has been widely adopted. In the VOF model, the sum of the volume fractions of all fluids inside any cell of the jet equals to one as described in eq. (4) where α_q is the volume fraction of the q^{th} fluid inside a control volume:

$$\sum_{q=1}^{n} \alpha_q = 1 \tag{4}$$

If the volume fraction of the q^{th} fluid in a cell is denoted as α_q, the following scenarios are possible. When the cell is empty, with no traced fluid inside, the value of α_q is zero; when the cell is full, $\alpha_q = 1$; and when the interphasal interface cuts the cell, then $0 < \alpha_q < 1$. The volume fraction α_q is a discontinuous function, its value jumps from 0 to 1 when the argument moves into interior of traced phase. This paper uses the VOF model to track the jet surface.

The interface(s) between the phases is tracked by the solution of the continuity equation for the volume fraction of one or more phases. The volume fraction equation of the q^{th} fluid can be written as eq. (5) where ρ_q is the density of the q^{th} fluid. The $\vec{\text{v}}_a$ and α_q are the velocity vector and volume fraction of the q^{th} fluid, and $p = 1, 2,\ldots, n$ is the suffix of the fluids in the multiphase flow. The $\dot{m}_{pq}(\dot{m}_{qp})$ is the mass transfer from phase $q(p)$ to phase $p(q)$. Equation (5) describes the volume transfer of the q^{th} fluid in space and time domains of a control volume:

$$\frac{1}{\rho_q}\left[\frac{\partial}{\partial t}(\alpha_q \rho_q) + \nabla(\alpha_q \rho_q \vec{\text{v}}_q) = \sum_{p=1}^{n}(\dot{m}_{pq} - \dot{m}_{qp})\right] \tag{5}$$

In this study, the VOF model is used to track the jet surface. The model makes use of the two-fluid Eulerian model for a two-phase incompressible flow, where phase fraction equations are solved separately for each individual phase; hence, the equations for the phase fractions can be expressed as [10]:

$$\frac{\partial \alpha_q}{\partial t} + \nabla(\alpha_q \vec{\text{u}}) + \nabla[\alpha_q \vec{\text{u}}_r (1 - \alpha_q)] = 0 \tag{6}$$

where $\vec{\text{u}}_r = \vec{\text{u}}_l - \vec{\text{u}}_a$ is the vector of relative velocity, l and a are densities of liquid and air, respectively.

The material property of the control volume is approximated by the material properties of the fluids weighted averaged by their volume fractions as shown in eq. (7) where ξ_q and ξ are the material property of the q^{th} fluid and the representative material property of the control volume, respectively:

$$\xi = \sum_{q=1}^{n} \alpha_q \xi_q \tag{7}$$

Similar to the material property, the velocity field is also shared among the fluids within the control volume. It is solved by a single momentum equation as shown in eq. (8) where p is the pressure and $\vec{g}$ is the gravitational force. It describes that the change of momentum in space and time domains equals to the sum of the forces including the differential pressure, shear stress and gravitational force acting on the control volume.

$$\frac{\partial}{\partial t}(\rho\vec{v}) + \nabla(\rho\vec{v}\vec{v}) = -\nabla p + [\mu(\nabla\vec{v} + \nabla\vec{v}^T)] + \rho\vec{g} \tag{8}$$

Numerical simulation method

According to the two-phase flow model presented, a standard finite-different interpolation schemes and the explicit approach are used to the volume fraction equation. The face values of the volume fraction are interpolated by using geometric reconstruction scheme. A standard k-ε model is used to model the turbulent viscosity. The two-phase flow in the single-bubble electrospinning process will be modeled by CFD.

Computational domain

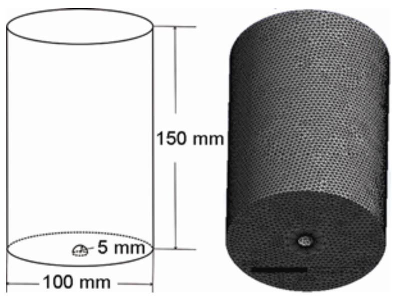

Figure 2. Computational domain and mesh generation

Figure 2 shows the flow domain used in the 3-D simulation for a reference case, a circular cylinder with diameter D = 100 mm and height h = 150 mm. In this case, the nozzle-to-collection distance is 150 mm, and the applied voltage is 15 kV. The air bubble nozzle's internal diameter is 10 mm. The diameter of single bubble is 10 mm, and the diameter of the initial jet produced is 2 mm. For the investigated 10 wt.% poly(lactic acid) solution the simulations shown were performed for the following process parameters: surface tension γ = 0.07 N/m, dynamic viscosity μ = 180 mPa·s, mass density ρ = 1000 kg/m^3, and initial jet velocity v = 10 m/s [9-10].

Boundary conditions

There are three boundaries, as shown in fig. 2. Each boundary was set as follows: flow inlet, free surface, and no-slip boundary condition:

– flow inlet: v_{in} = 10 m/s,
– free surface: zero normal gradient $\partial ø/\partial n = 0$ for all variables, and
– no-slip boundary: zero velocity relative to the wall ($v_{\text{wall}} = 0$).

Results

The motion of the jet can be traced by the streamline plots in fig. 3. Figure 4 shows the experimental data. It can be seen that the numerical simulation results correspond well to the experimental data.

In this numerical simulation, we only simply simulated the single-bubble electrospinning instability process using CFD. In future, we will take into account the deformation of bubble and multi-bubbles, which play pivotal roles in determining the nanofiber yield.

Conclusion

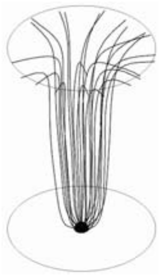

Figure 3. The motion of the jets

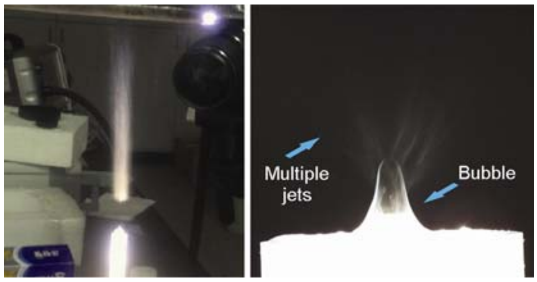

Figure 4. Distribution of the jet velocity

This paper deals with studying numerically the two-phase flow in the bubble-electrospinning process by applying CFD techniques for gaining significant insight into understanding of its mechanical mechanism. The calculation results are reasonable and reliable. That means the CFD method is a powerful approach to research mechanical mechanism of the bubble-electrospinning process and it is very important for the development of bubble-electrospinning.

Acknowledgment

The work is supported financially by PAPD (A Project Funded by the Priority Academic Program Development of Jiangsu Higher Education Institutions), Jiangsu Provincial Natural Science Foundation of China (Grant No. BK20131175), Natural Science Foundation of the Jiangsu Higher Education Institutions of China (Grant No. 14KJA130001), Suzhou Science and Technology Project (Grant No. SYG201434), and Nantong Science and Technology Project (Grant No. BK2014050).

References

[1] He, J.-H., Effect on Temperature on Surface Tension of a Bubble and Hierarchical Ruptured Bubbles for Nanofiber Fabrication, *Thermal Science*, *16* (2012), 1, pp. 327-330
[2] He, J.-H., *et al.*, BioMimic Fabrication of Electrospun Nanofibers with High-Throughput, *Chaos, Solitons and Fractals*, *37* (2008), 3, pp. 643-651
[3] He, J.-H., *et al.*, Review on Fiber Morphology Obtained by Bubble Electrospinning and Blown Bubble Spinning, *Thermal Science*, *16* (2012), 5, pp. 1263-1279
[4] Dong, L., *et al.*, Mathematical Model of Electric Field Distribution at a Critical State in Bubble Electrospinning, *Fiber Bioengineering and Informatics*, *3* (2010), 2, pp. 117-120
[5] Wilson C., *et al.*, The Bursting of Soap Bubbles in an Uniform Electric Field, *Mathematical Proceedings of the Cambridge Philosophical Society*, *22* (1925), 5, pp. 728-730
[6] Xu, L., *et al.*, Numerical Simulation of a Two-Phase Flow in the Electrospinning Process, *International Journal of Numerical Methods for Heat & Fluid, 24* (2014), 8, pp. 1755-1761
[7] Hu, Y. Y., *et al.*, Numerical Study on Two-Phase Flow Patterns in Coaxial Electrospinning, *Journal of Applied Physics, 101* (2007), ID 084307
[8] Gopala, V. R., *et al.*, Volume of Fluid Methods for Immiscible-Fluid and Free-Surface Flows, *Chemical Engineering Journal, 141* (2008), 1-3, pp. 204-221
[9] Yeoh, G. H., *et al.*, *Computational Techniques for Multiphase Flows*, Elsevier Ltd., Oxford, UK, 2010
[10] Wei, W., *et al.*, Numerical Simulation of the Cone-Jet Formation and Current Generation in Electrostatic Spray-Modeling as Regards Space Charged Droplet Effect, *Journal of Micromechanics and Microengineering, 23* (2013), 1, ID 015004

Paper submitted: January 15, 2015
Paper revised: March 10, 2015
Paper accepted: April 30, 2015